The Molecular and Electronic Structure of Tetrasulphur-dinitride; a Study by ab initio Molecular Orbital Methods and Photoelectron Spectroscopy

Michael H. Palmer
Department of Chemistry, University of Edinburg, Edinburgh, Scotland

Woon Ming Lau and Nicholas P. C. Westwood
Department of Chemistry*, University of British Columbia, Vancouver, Canada

Z. Naturforsch. **37a**, 1061 – 1067 (1982); received May 18, 1982

The He(I) photoelectron spectrum of gaseous S_4N_2 is reported, and an assignment is made on the basis of the correlation with ab initio molecular orbital calculations. The latter, based upon the recently optimised geometry of C_S symmetry, used both a large basis set of greater than double zeta quality, together with configuration for both the ground state and the ionised states. The Koopmans' Theorem order gives a reasonable prediction of the order of states for most of the low energy ionised states; beyond IP_5 additional states involving excitation processes in conjunction with ionisation were computed. The numerical agreement between the observed IP's and the CI value is reasonable.

Introduction

Although a series of isomeric structures can be drawn for S_4N_2, a single substance of this formula has been obtained from a variety of reactions [1 – 4]. Most evidence pointed to a 6-membered ring with the nitrogen atoms in a meta orientation, but there was support for both planar and non-planar structures [2, 3]. Recently we reported a full geometry optimisation of the molecule by an *ab initio* gradient method using both C_{2V} (planar) and C_S symmetry (non-planar structures) [5]; the latter was found to be significantly lower in energy, hence much more probable. Concurrently, and after our paper was submitted, a study by Chivers et al. [6] was published which confirmed the crystal structure as non-planar (C_S); the structures from References [5] and [6] are very similar. We concluded [5] that (i) the molecule was reasonably well by **1** on the basis of a localised orbital transformation; (ii) that only in the N = S = N unit did the $3d_S$ orbitals have any significant population; (iii) although overall the 4 sets of $3d_S$ orbitals led to a significant lowering of total energy, almost all of this arises from the implicit extra 3s orbital contained within the 6 Cartezian Gaussian functions $(3d_X2 + 3d_Y2 + 3d_Z2 = 3d_R2 = 3\text{s-orbital})$; we have referred to this on a number of previous occasions [7].

We now wish to report the He(I) UV-photoelectron spectrum of S_4N_2; the facile decomposition of this molecule meant that monitoring by mass spectrometry during the photoelectron data (PE) collection was essential. We have computed a number of electronic states for S_4N_2 ions of both A' and A'' symmetry, as well as the ground state; these calculations used a further improved wavefunction (relative to [5]), and large scale configuration interaction (CI) of the various states. Thus the study does *not* rely upon Koopmans' Theorem (KT) studies of the ground state wavefunction (GS), although a comparison with this has been performed.

Methods

(a) Synthesis of S_4N_2

This difficult process was achieved by reaction of methanolic S_7NH, heptasulfurimide, with mercury-(II)acetate [8]. The resulting precipitate was filtered, washed and dried in vacuo, and maintained at 0 °C in vacuo. The pure compound was fractionally sublimed from the above mixture and identified by combined mass spectrometry and PE spectroscopy as described below.

---

* 2036 Main Mall, Vancouver V6T1Y6.

Reprint requests to Dr. M. H. Palmer, Department of Chemistry University of Edinburgh, West Mains Road, Edinburgh EH9 3JJ, Schottland.

0340-4811 / 82 / 0900-1061 $ 01.30/0. — Please order a reprint rather than making your own copy.

A sample of the mixture, at −78 °C, was carefully allowed to warm in a gas line attached directly to the spectrometer. The products were analysed by their PE and mass spectra, and were found to consist of S_4N_2 together with S_2N_2. The principal contaminant S_2N_2, could be removed at temperatures below −15° and was identified by its PE spectrum [9, 10]. By careful evaporation between −15° and 0 °C, S_4N_2 was obtained as dark red needle-like crystals, m.p. ∼20°.

(b) Combined Photoelectron and Mass Spectral Measurements

The PE spectrometer was basically as previously described [11], but with a modification consisting of an einzel lens to raise the photoionisation position and permit coupling to an *in-situ* quadrupole mass spectrometer. The complete system is under the control of an LSI 11/03 mini-computer. Although the PE and mass spectra are not collected in coincidence, the instrumental arrangement allowed switching between the two modes over a few seconds, and well within the collecting time of the PE spectra. Unlike many PE spectrometers, the instruments does not discriminate against low kinetic energy electrons, and hence a rising background occurs to high binding energy. The He(I) PE spectra and mass spectra recorded with different light sources are shown in Figs. 1 and 2, and the ionisation potentials are recorded in Table 1. The MS taken with different ionisation sources demonstrates the purity of the sample and the changes in cracking pattern facilitate this process. This technique provides an invaluable aid to determining the nature of unknown transient species, particularly in a mixture [11 a]. No peaks with m/e greater than 156 were observed.

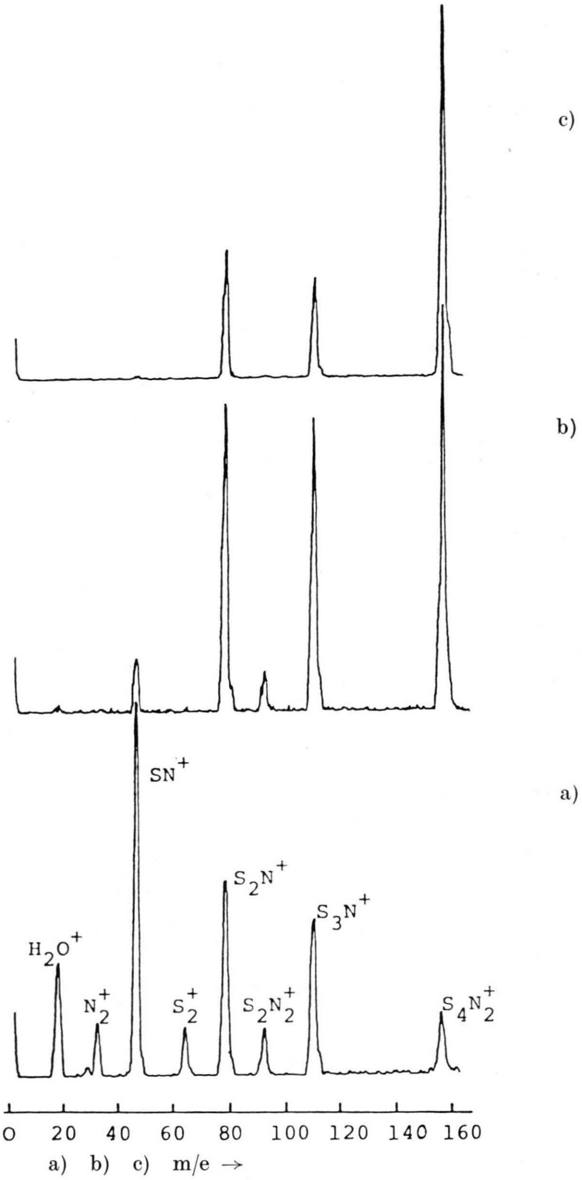

Fig. 1. (a) HeI quadrupole mass spectrum of S_4N_2; (b) $HL_{\alpha,\beta,\gamma}$ (unfiltered) quadrupole mass spectrum of S_4N_2; (c) HL_α (filtered LiF) quadrupole mass spectrum of S_4N_2.

(c) Computational Methods

The same linear combination of Gaussian orbital basis (LCGO) as in our previous papers [5, 12] was used for sulfur; this is a S(12s9pld) basis contracted to S[7s4pld]; it is thus better than double zeta (ns, ns', np, np') in s-functions, having an additional $3s''$ as well as implicit $3s'''$ from the d-functions. The nitrogen basis was Dunning's double zeta basis [13].

Table 1. Ionization Potentials of S_4N_2 (all peaks ± 0.02 eV band maxima).

Peak	1	2	3	4	5	6	7	8	9	10	11
IP (eV)	8.58	9.38	10.72	11.06	12.10	12.50	13.23	14.49	15.51	16.75	17.47

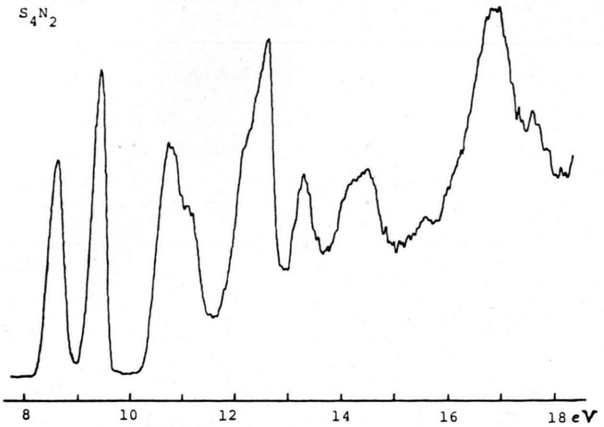

Fig. 2. HeI photoelectron spectrum of S_4N_2.

The computations were carried out on CDC 7600 and CRAY-1 computers using the ATMOL-3/SPLICE system of programs [14]. In view of the large number of electron repulsion integrals generated (7 × 2400 ft of magnetic tape at 1600 BPI), it was necessary to carry out the CI study on a sub-set of the largest spd-basis calcusation. Hence the total energy lowering by the CI is less than could be obtained, and has to be seen as relative to the sp-basis set calculation, although 3d functions were retained in the 'active orbital' set. In the first phase of CI, the 7 highest occupied MO's together with the lowest 17 virtual orbitals were active; this was then extended to 10 occupied plus 17 virtual orbitals. All single and double excitations within the 24 (or 27) active orbitals were included; configuration selection based upon a perturbation selection process was employed with varying levels of selection criterion [15] if necessary. In the case of the ground state it was possible to avoid any selection since the number of configurations was sufficiently small. Thus the 14 electron (24 active) case gave 3669

Table 3. Orbital and Total Energies for S_4N_2: Single Configuration.

Total Energy — 1698.89987 a.u.
Virial Theorem (V/T) — 2.000045
Orbital Energies (eV)

a'	10.18	12.00	13.65	14.04	16.65	17.31
	19.64	25.45	30.15	33.38		
a''	9.14	11.61	13.78	14.71	18.62	26.13

Table 4. Mulliken Analysis (a) Occupied Set, (b) Virtual Set used in the Configuration Interaction Study.

(a) *Occupied Set*				
Orbital	Sl	S 3/S 5	S 4	N 2/N 6
23	37.12	9.25	1.04	52.58
24	12.50	20.08	0.08	65.42
25	11.59	45.00	39.37	4.04
26	12.87	63.13	5.74	18.24
27	18.61	24.00	36.38	21.02
28	20.23	45.40	17.56	16.83
29	13.19	37.02	14.50	35.27
30	30.36	16.34	7.62	45.67
31	39.74	8.90	5.39	45.96
32	2.22	59.38	11.65	26.72
33	34.24	30.92	18.42	16.41
34	3.57	33.60	0.45	62.36
35	5.12	38.77	40.58	15.52
36	13.88	28.17	45.20	12.74
37	4.41	23.18	15.98	56.41
38	7.13	47.20	41.65	4.00
39	3.19	60.19	0.83	35.78
(b) *Virtual Set*				
40	42.81	11.26	4.41	41.48
41	12.97	46.54	31.14	9.35
42	8.77	38.42	43.98	8.82
43	11.41	69.68	19.57	0.68
44	26.15	57.69	1.81	14.35
45	28.46	48.05	2.32	1.16
46	39.23	48.76	−0.81	12.81
47	96.26	23.97	3.22	−23.45
48	4.54	93.82	3.44	− 1.82
49	65.51	33.46	7.90	− 6.87
50	3.78	39.88	56.84	− 0.50
51	40.04	6.89	45.76	7.30
52	3.83	54.23	41.90	− 0.17
53	52.87	16.37	27.38	1.69
54	23.47	65.63	10.89	0.00
55	26.09	74.34	0.39	− 0.82

Table 2. The Ground State Configuration Interaction Studies.

No. of Active Orbitals		Number of Configurations	Total Energy	Comments
Occupied	Virtual			
39	0	1	— 1698.89987	Initial Calculation Full Spd basis (120)
7	17	1	— 1698.80345	Reference Configuration
7	17	841	— 1698.89359	Selection at 30 μH
7	17	1264	— 1698.89852	Selection at 15 μH
7	17	3669	— 1698.91036	Energy Lowering by CI is 0.10691 a.u. No selection
10	17	1314	— 1698.92736	Selection at 30 μH
10	17	2068	— 1698.93569	Selection at 15 μH
10	17	7426		No selection

Table 5.

Configuration Number	Eigenvector[a]	Orbital Occupancy[b]
(a) Ground State — 20 Active Electrons — 27 Active Orbitals		
1	0.9431	$(5a')^2$ to $(10a')^2$, $(4a'')^2$ to $(7a'')^2$
2	−0.0831	$(5a')^2$, $(6a')^2$, $(4a'')^2$ to $(7a'')^2$, $(8a')^2$ to $(10a')^2$, $(7a', 13a')$
3	−0.0702	$(5a')^2$ to $(10a')^2$, $(4a'')^2$ to $(6a'')^2$, $(11a')^2$
4	0.0631	$(5a')^2$ to $(8a')^2$, $(4a'')^2$ to $(7a'')^2$, $(10a')^2$, $(9a', 13a')$
5	0.0581	$(5a')^2$ to $(11a')^2$, $(4a'')^2$, $(5a'')^2$, $(6a'', 7a'')$
6	0.0569	$(6a')^2$ to $(10a')^2$, $(4a'')^2$ to $(7a'')^2$, $(5a', 13a')$
7	−0.0564	$(5a')^2$, $(6a')^2$, $(4a'')^2$ to $(7a'')^2$, $(8a')^2$ to $(10a')^2$, $(7a', 12a')$
8	0.0555	$(5a')^2$, $(6a')^2$, $(4a'')^2$ to $(7a'')^2$, $(8a')^2$ to $(10a')^2$, $(7a', 15a')$
9	−0.0502	$(5a')^2$ to $(7a')^2$, $(4a'')^2$ to $(7a'')^2$, $(9a')$, $(10a')^2$, $(8a', 13a')$
(b) Ground State — 14 Active Electrons — 24 Active Orbitals		
1	0.9450	$(7a')^2$, $(5a'')^2$, $(8a')^2$, $(9a')^2$, $(6a'')^2$, $(10a')^2$, $(7a'')^2$
2	−0.0811	$(5a'')^2$, $(8a')^2$, $(9a')^2$, $(6a'')^2$, $(10a')^2$, $(7a'')^2$, $(7a', 13a')$
3	−0.0806	$(7a'')^2$, $(5a'')^2$, $(8a')^2$, $(9a')^2$, $(6a'')^2$, $(10a')^2$, $(11a')^2$
4	0.0638	$(7a')^2$, $(5a'')^2$, $(8a')^2$, $(6a'')^2$, $(10a')^2$, $(7a'')^2$, $(9a', 13a')$
5	0.0631	$(7a')^2$, $(5a'')^2$, $(8a')^2$, $(9a)^2$, $(10a')^2$, $(11a')^2$, $(6a'', 7a'')$
6	0.0606	$(5a'')^2$, $(8a')^2$, $(9a')^2$, $(6a'')^2$, $(10a')^2$, $(7a'')^2$, $(7a', 15a')$
7	−0.0566	$(5a'')^2$, $(8a')^2$, $(9a')^2$, $(6a'')^2$, $(10a')^2$, $(7a'')^2$, $(7a', 12a')$
8	−0.0542	$(7a')^2$, $(5a'')^2$, $(9a')^2$, $(6a'')^2$, $(10a')^2$ $(7a'')^2$, $(8a', 13a')$

[a] All other configurations have eigenvector less than 0.0500.

[b] Valence shell numbering only, from $1a'$ to $1a''$ upwards. Paired functions in parentheses. To facilitate comparison, the ground state single configuration (Number 1) canonical order is retained as far as possible.

configurations, and the 20 electron (27 active) case gave 7426 configurations. The energies, numbers of configurations and principal components of the CI vectors for both ground and ionised states are shown in Tables 2 – 5.

For convenience in numbering, we label orbitals from high to low binding energy, but in the valence shell *only;* we refer to all orbitals, occupied or virtual, that are not in the CI expansion as 'frozen'; this category includes all core electrons and some inner valence levels.

Results and Discussion

(a) The Ground State Wave-Function

The starting point for the present work was the optimal geometry found in our earlier paper [5]; the total energy of the C_S symmetry state was subsequently improved, and this together with the valence shell orbital energies is given in Tables 2 and 3. It will be seen that the virial theorem is still further improved over [5], and is now effectively at the theoretical limit of $-2.0000^{\cdot}$. The orbital energies basically show similar ordering to those in [5]; however, the relative spacings are now much more easily recognisable in terms of the experimental spectra via Koopmans' Theorem. Indeed, if the present orbital energies are multiplied by 0.92 (as is often done), then the first 9 orbital energies are effectively identical to the observed IP's. The atomic populations for the single configuration calculation are shown in Table 4, these contain the orbitals from which the CI was performed.

In the first phase of CI, the active set of orbitals consisted of the set $7a'-10a'$, $5a''-7a''$ (all doubly occupied) and the virtual set $11a'-21a'$, $8a''-14a''$, a total of 24 orbitals. The ground state calculation yielded a total of 3669 configurations, all of which were included in the CI.

When the number of 'active' orbitals was increased by three, the number of possible configurations rose to 7426. Although this set was calculated, the effect upon most of the properties was negligible (Table 5). Also, it was clear that some level of configuration selection would be necessary for the ionised states; these 'selected' results are also shown in Table 2. A comparison of the principal components of the CI vector for the two 'active' sets shows that for *all configurations* with an eigenvector greater than ± 0.05, only one new configuration (Number 6) appears in the larger calculation (Table 5); it involves excitation from orbital $5a'$ which is frozen in the smaller calculation, and thus can only appear in the larger one. All other 8 configurations of major proportion are present at both levels of CI, and that suggests that the basis is large enough to draw firm conclusions. The only valence shell orbitals omitted from the CI at this point are orbitals $1a'$ to $4a'$ and $1a''$ to $3a''$; this group of 7 orbitals are largely $2s_N$ and $3s_S$ in character (Table 4). We can expect a considerable lowering of energy to be obtained when they are included, but their importance to the outer valence shell IP's, of primary importance to the present work can be regarded as minimal.

The first major conclusion is that the CI energy lowering of the ground state (Table 2) is relatively modest, and this is a result of the final natural orbitals being dominated (90%) by the initial single configuration (Table 5). The principal excited configurations are of three basic types; with ground state single configuration orbitals ("bonded-functions", $\langle aa \rangle$ or $\langle bb \rangle$ yielding (i) $\langle aj \rangle$, (ii) $\langle jj \rangle$, and (iii) $\langle jk \rangle$ where j and k come from the virtual set. Only 6 out of the largest 50 contributors are of type (ii), although this includes the 3rd largest configuration. In fact 19 of this group are single replacements of type (i), often in the form $\langle aa \rangle \langle bb \rangle \rightarrow \langle aj \rangle \langle bk \rangle$. Most of the configurations are strongly delocalised, the principal exceptions being configurations 3 and 5, both of which are concerned with excitation into the $N=S=N$ π^* and σ^* system.

(b) Ionised States by Configuration Interaction

Using the 'active' orbital basis of 14 and 20 electrons we can identify a series of principal ionised states of A' and A'' symmetry (Table 6). Thus vacancies can be envisaged in any one of the occupied orbitals $5a'$ to $10a'$ and $4a''$ to $7a''$. These 'ionised states' formed the 'root functions' for the CI study, and all single and double excitations from these root functions were considered. Thus as well as obtaining energies for the root function dominated states, we can except to compute a number of processes arising from shake-up and shake-off phenomena [16].

The use of the sets of root functions (Table 6) even with the larger orbital basis (i.e. with $5a'$, $6a'$ and $4a''$ included) led to a large number of configurations (53816 and 46120 for A' and A''). It was thus necessary, for computational reasons, to truncate these lists, in order to eliminate the smaller contributors to the energy. This was done by perturbation energy selection, whith configurations contributing 30 and 15 micro-Hartree being retained in two levels of CI for both A' and A'' states.

Table 6. Root Functions for the Ionised States.

State Symmetry	Orbital Vacated[a]					
A'	$5a'$	$6a'$	$7a'$	$8a'$	$9a'$	$10a'$
A''	$4a''$	$5a''$	$6a''$	$7a''$		

[a] The full root functions can be constructed by comparison with the ground state function, Configuration 1 of Table 5 (a). Thus 6 root functions of A' and 4 of A'' symmetry were used.

The most immediate observation (Table 7) was that the three lowest A'' states and two lowest A' states are dominated by the initially selected root functions (Table 6); that is, the state is basically associated with ionisation from a single orbital. Furthermore, these are in the KT order, and have energies and spacing very similar to that of KT. Whilst KT has become rather unfashionable, and clearly requires verification in a number of CI studies to determine whether trends in its accuracy are apparent, it would seem imprudent to over-exaggerate its failings. The present first 5 IP's are a very successful demonstration of its power and value. Beyond the 5th IP the position becomes more complex; the 3rd, 4th, 5th and 6th A' states are linear combinations of basically two, three, two and one terms respectively; the $3A'$ and $5A'$ states are over 50% of the root function, having $8a'$ and $7a'$ vacated, but both are very heavily contaminated with a shake-up phenomenon (Table 7). The position with state $4A'$ is more complex, being largely a linear combination of 3 roots in which ionisation from both $8a'$ and $10a'$ is accompanied by the same shake-up phenomenon. The next state, $6A'$ reverts to a more simple type and is a shake-up state, but different from the previous one. In all, with some 12 ionised states computed, it is still possible to recognise most of these as associated with ionisation from a particular orbital.

(c) Assignment of the Photoelectron Spectrum

The present basis set, and the level of CI is sufficiently large that it is reasonable to correlate the observed IP's directly with the electronic states observed. There is one major reservation however; since we at present cannot calculate the cross-sections associated with particular states, we cannot be sure which states will be of high or low intensity. We initially adopt the view that the latter can be assigned to states which are clearly identified as linear combinations of apparent shake-up roots, and that the more intense lines are states in which a 'pure' ionisation without excitation configuration is at least pronounced, and often dominant. Depending upon the sharpness of the IP peak envelope we then

Table 7. Ionised Electronic States Computed by Configuration Interaction and Correlation with the Photoelectron Spectrum.

Symmetry	Energy (+1698.0)	Ionisation Potential Calculated (eV)	Eigenvector (unnormalised)	Wave-function Occupancy (Root Function)	Ionisation Potentials observed (eV)	Interpretation
A''	-0.57276	8.730	0.94	$(7a')^2 (5a'')^2 (8a')^2 (9a')^2 (6a'')^2 (10a')^2 \quad (7a'')^1$	8.58	Ionisation
A'	-0.53883	9.653	0.93	$(7a')^2 (5a'')^2 (8a')^2 (9a')^2 (6a'')^2 (7a'')^2 \quad (10a')^1$	9.38	Ionisation
A''	-0.44931	12.089	0.94	$(7a')^2 (5a'')^2 (8a')^2 (9a')^2 (10a')^2 (7a'')^2 \quad (6a'')^1$	10.72	Ionisation
A'	-0.43577	12.458	0.93	$(7a')^2 (5a'')^2 (8a')^2 (6a'')^2 (10a')^2 (7a'')^2 \quad (9a')^1$	11.06	Ionisation
A''	-0.39591	13.542	0.81	$(7a')^2 (8a')^2 (9a')^2 (6a'')^2 (10a')^2 (7a'')^2 \quad (5a'')^1$	12.10	Ionisation
			0.34	$(7a')^2 (5a'')^2 (8a')^2 (9a')^2 (6a'')^2 (10a', 11a') (7a'')^1$		+ shake-up
A'	-0.38355	13.879	0.69	$(7a')^2 (5a'')^2 (9a')^2 (6a'')^2 (10a')^2 (7a'')^2 \quad (8a')^1$	12.50	Ionisation
			0.57	$(7a')^2 (5a'')^2 (8a')^2 (9a')^2 (6a'')^2 (10a')^2 \quad (11a')^1$		+ shake-up
A''	-0.37214	14.189	0.41	$(7a')^2 (5a'')^2 (8a')^2 (9a')^2 (6a'')^2 (10a', 11a') (7a'')^1$	13.23	Shake-up+ Ionisation
			0.40	$(7a')^2 (5a'')^2 (8a')^2 (9a')^2 (6a'')^2 (10a', 7a'') (11a')^1$		
			0.38	$(7a')^2 (8a')^2 (9a')^2 (10a')^2 (6a'')^2 (7a'')^2 \quad (5a'')^1$		
A'	-0.36402	14.410	0.58	$(7a')^2 (5a'')^2 (9a')^2 (6a'')^2 (10a')^2 (7a'')^2 \quad (8a\ )^1$	~ 14.1	Ionisation
			0.52	$(7a')^2 (5a'')^2 (8a')^2 (9a')^2 (6a'')^2 (10a')^2 \quad (11a')^1$		+ shake-up
			0.44	$(5a'')^2 (8a')^2 (9a')^2 (6a'')^2 (7a'')^2 (7a', 11a') (10a')^1$		
A'	-0.35120	14.759	0.80	$(5a'')^2 (8a')^2 (9a')^2 (6a'')^2 (10a')^2 (7a'')^2 \quad ((7a')^1$	14.49	Ionisation
			0.40	$(7a')^2 (5a'')^2 (8a')^2 (9a')^2 (6a'')^2 (10a')^2 \quad (11a')^2$		+ shake-up
A''	-0.34366	14.964	0.65	$(7a')^2 (5a'')^2 (8a')^2 (9a')^2 (6a'')^2 (10a', 11a') (7a'')^1$	$\sim 15 - 16$	Shake-up
			0.63	$(7a')^2 (5a'')^2 (8a')^2 (9a')^2 (6a'')^2 (10a', 7a'') (12a')^1$		
			0.57	$(7a')^2 (5a'')^2 (8a')^2 (9a')^2 (6a'')^2 (10a', 7a'') (11a')^1$		
			0.51	$(7a')^2 (5a'')^2 (8a')^2 (9a')^2 (6a'')^2 (10a', 12a') (7a'')^1$		
A'	-0.32283	15.531	0.82	$(7a')^2 (5a'')^2 (8a')^2 (6a'')^2 (10a')^2 (7a'', 8a'') (9a')^1$	$\sim 15 - 16$	Shake-up
			0.26	$(7a')^2 (5a'')^2 (8a')^2 (6a'')^2 (10a')^2 (7a'', 8a'') (9a')^1$		
A'	-0.31623	17.711	0.97	$(7a')^2 (5a'')^2 (8a')^2 (9a')^2 (6a'')^2 (7a'', 8a'') (10a')^1$	$\sim 15 - 16$	Shake-up
			0.65	$(7a')^2 (5a'')^2 (8a')^2 (9a')^2 (6a'')^2 (10a', 7a'') (8a'')^1$		

group states accordingly; the final assignments to observed IP's are shown in Table 7.

The first 4 IP's are effectively pure excitations from a ground state orbital, and are thus explicitely of the KT or 'one particle' type of process. The symmetries, and indeed the computed energies of these states are just as well predicted by KT as by the CI study. However, it is clear that shake-up phenomena occur at very low ionisation potentials, indeed the first example here is at ~ 12 eV. Thus even at such a low binding energy KT shows indications of breakdown; this is much lower than is often ascribed to related cyclic compounds such as S_2N_2 (14.7 eV) [17], aromatic molecules (18 eV) [18] and other hydrocarbons (21 eV) [19].

Conclusions

In this paper, our first in a series on large scale CI of polyatomic cyclic molecules, we have shown that KT with a very large basis gives values for IP's nearly as satisfactorily as does even large scale CI with up to 7000 configurations. Of course where more symmetry representations are present, the correct sequencing of these IP's will be more difficult, and hence KT may well break down more quickly. The occurrence of shake-up phenomena at IP's as low as 12 eV is unusual, but may be associated with the number of second row atoms and lone pairs orbitals in this molecule; S_4N_2 is of course strongly coloured.

In most instances (in fact for the first five states involving shake-up), the LUMO ($11a'$) plays the key role. This is another example (see e. g. CH_3NO, N_2O_4 [11 a]) where a low-lying unoccupied orbital, in this case π^*, causes a breakdown of the one particle picture, and manifests itself as weak satellite structure in the photoelectron spectrum. It behoves PE spectroscopists to no longer consider weak structure in their spectra as impurities etc., but to consider possible multi-particle process (breakdown of the quasiparticle picture) instead.

Acknowledgements

The authors wish to thank the following for interest and encouragement: Professor C. A. McDowell, Dr. N. L. Paddock, Dr. D. C. Frost (all U.B.C., Vancouver, Canada), and Dr. M. F. Guest (Daresbury Laboratory, England).

[1] H. G. Heal, The Inorganic Heterocyclic Chemistry of Sulfur, Nitrogen and Phosphorus, Academic Press, London 1980, p. 115, Chapter 6.

[2] A. J. Banister, Nature London **237**, 92 (1972).

[3] W. L. Jolly, Sulfur Research Trends, Adv. Chem. Ser. **110**, 9 (1972).

[4] H. W. Roesky, Angew. Chem. Int. Ed. **18**, 91 (1979).

[5] M. H. Palmer, J. R. Wheeler, R. H. Findlay, N. P.C. Westwood, and W. M. Lau, J. Molec. Struct. (Theochem.) **86**, 193 (1981).

[6] T. Chivers, P. W. Codding, and R. T. Oakley, J. Chem. Soc. Chem. Comm. **1981**, 584

[7] M. H. Palmer and R. H. Findlay, Tetrahedron Letters **1972**, 4165; J. Chem. Soc. Perkin Trans. II **1974**, 1885; M. H. Palmer, R. H. Findlay, W. Moyes, and A. J. Gaskell, J. Chem. Soc. Perkin Trans. II, **1975**, 841.

[8] H. G. Heal and R. J. Ramsay, J. Inorg. Nucl. Chem. **37**, 286 (1975).

[9] D. C. Frost, M. R. LeGeyt, N. L. Paddock, and N. P. C. Westwood, J. Chem. Soc. Chem. Comm. **1977**, 217.

[10] R. H. Findlay, M. H. Palmer, A. J. Downs, R. G. Egdell, and R. Evans, Inorg. Chem. **19**, 1307 (1980). Note that in this reference line 6 of the Section "Computational Methods" should read "S[7 s 4 p]" as in the present work.

[11] W. M. Lau, Ph. D. Thesis, U. B. C. 1981; D. C. Frost, S. T. Lee, C. A. McDowell, and N. P. C. Westwood, J. Electron Spectrosc. **12**, 95 (1977).

[12] M. Redshaw, M. H. Palmer, and R. H. Findlay, Z. Naturforsch. **34 A**, 220 (1979).

[13] T. Dunning, J. Chem. Phys. **53**, 2823 (1970).

[14] B. T. Sutcliffe, J. Chem. Phys. **45**, 235 (1966); G. H. F. Diercksen and B. T. Sutcliffe, Theoret. Chim. Acta **34**, 105 (1974).

[15] M. F. Guest and W. R. Rodwell, The Bonded Function CI Program, Science Research Council, Atlas Computing Division, September 1977; RL-77-110/B.

[16] K. Siegbahn, C. Nordling, G. Johansson, J. Hedman, P. F. Heden, K. Hamrin, U. Gelius, T. Bergmark, L. O. Werme, R. Manne, and Y. Baer, ESCA Applied to Free Molecules, North Holland, Elsevier, Amsterdam 1971, Chapt. 5 **ff**.

[17] W. von Niessen and G. H. F. Diercksen, J. Electron Spectrosc. **20**, 95 (1980).

[18] W. von Niessen, G. H. F. Diercksen, and L. S. Cederbaum, Chem. Phys. Letters **45**, 295 (1977).

[19] W. von Niessen and G. H. F. Diercksen, J. Electron Spectrosc. **16**, 351 (1979).